Title: Motor unit dysregulation following 15 days of unilateral lower limb immobilisation

Running title: Neural dysregulation with muscle disuse

Thomas B. Inns[1], Joseph J. Bass[1], Edward J.O. Hardy[1, 2], Daniel J. Wilkinson[1], Daniel W. Stashuk[3], Philip J. Atherton[1], *Bethan E. Phillips[1], *Mathew Piasecki[1]

[1]Centre Of Metabolism, Ageing & Physiology, MRC-Versus Arthritis Centre for Musculoskeletal Ageing Research and NIHR Nottingham BRC, University of Nottingham, Derby, UK. [2]Department of Surgery and Anaesthetics, Royal Derby Hospital, Derby, UK. [3]Department of Systems Design Engineering, University of Waterloo, Ontario, Canada. (*Co-senior authorship).

Corresponding author: mathew.piasecki@nottingham.ac.uk

Key words: Muscle disuse, electromyography, NMJ, motor unit

Key points

- Muscle mass and function decline rapidly in situations of disuse such as bed rest and limb immobilisation.
- The reduction in muscle function commonly exceeds that of muscle mass, which may be associated with the dysregulation of neural input to the muscle.
- We have used intramuscular electromyography to sample individual motor unit and near fibre potentials from the vastus lateralis following 15 days of unilateral limb immobilisation. Following disuse, the disproportionate loss of muscle strength when compared to size was associated with suppressed motor unit firing rate and increased markers of neuromuscular junction transmission instability.
- These central and peripheral motor unit adaptations were observed at multiple contraction levels and in the immobilised limb only. Our findings demonstrate neural dysregulation as a key component of functional loss following muscle disuse in humans.

Abstract

Disuse atrophy, caused by situations of unloading such as limb immobilisation, causes a rapid yet diverging reduction in skeletal muscle function compared to muscle mass. While mechanistic insight into the loss of mass is well studied, deterioration of muscle function with a focus towards the neural input to muscle remains underexplored. This study aimed to determine the role of motor unit adaptation in disuse-induced neuromuscular deficits. Ten young, healthy male volunteers underwent 15 days of unilateral lower limb immobilisation with intramuscular EMG (iEMG) recorded from the vastus lateralis during knee extensor contractions normalised to maximal voluntary contraction (MVC) pre and post disuse. Muscle cross-sectional area was determined by ultrasound. Individual MUs were

sampled and analysed for changes in MU discharge and MU potential (MUP) characteristics. Vastus lateralis (VL) CSA was reduced by approximately 15% which was exceeded by a two-fold decrease of 31% in muscle strength in the immobilised limb, with no change in either parameter in the non-immobilised VL. Parameters of MUP size were largely reduced with immobilisation, while neuromuscular junction (NMJ) transmission instability increased, and MU firing rate decreased at several contraction levels. All adaptations were observed in the immobilised limb only. These findings highlight impaired neural input following immobilisation reflected by suppressed MU discharge rate and instability of transmission at the NMJ which may underpin the disproportionate reductions of strength relative to muscle size.

Introduction

Disuse atrophy is the loss of skeletal muscle mass associated with decreased external loading or complete immobilisation. It is common in clinical settings following joint trauma, nerve injury, or prescribed bed rest, and progresses rapidly with reductions of strength occurring after just 5 days (Wall *et al.*, 2014). As such, it has been widely applied as an experimental model to investigate underpinning mechanisms in scenarios of space flight, prolonged bed rest, spinal cord injury, and ageing (Castro *et al.*, 1999; Narici & De Boer, 2011; Puthucheary *et al.*, 2013). The trajectory of decline is not linear; five days of unilateral lower limb suspension lead to ~3 % reduction in quadricep cross-sectional area (CSA) (Wall *et al.*, 2014) and eight weeks of bed rest reduced quadriceps CSA by ~14% (Mulder *et al.*, 2006).

The loss of muscle strength with disuse is commonly reported to exceed the loss of muscle size. Following 8 weeks of bedrest, quadriceps CSA declined by 14% compared to a 17% decline in strength (Mulder *et al.*, 2006), while only 10 days of bed rest was enough to elicit a ~6% reduction in CSA and a ~14% reduction in knee extensor maximal voluntary contraction (MVC) (Monti *et al.*, 2021). Furthermore, meta-analysis of bed rest studies with a combined 118 participants across various durations of disuse found no relationship between length of bed rest and muscle size, whereas muscle power reduction and bed rest duration were strongly related (Di Girolamo *et al.*, 2021). Numerous data provide mechanistic insight to muscle *atrophy*, including decreased MPS, increased MPB, mitochondrial dysfunction, insulin resistance, and histochemical markers of fibre denervation (Phillips *et al.*, 2009; Rudrappa *et al.*, 2016; Monti *et al.*, 2021), yet mechanistic insight into loss of muscle *function* is less clear.

Successful activation of muscle relies upon coordinated input to the motoneuron pool and synaptic transmission across neuromuscular junctions (NMJs), with increases in muscle force mediated by the recruitment and rate modulation of functioning motor units (MUs). Motor units from hand muscles

showed a marked reduction in FR following disuse, which corresponded with reduced force generating capacity (Duchateau & Hainaut, 1990). Biopsies from the VL following 10 days of bed rest revealed structural disruption at the NMJ (Monti *et al.*, 2021) suggesting a contribution to decreased muscle activation and function. Furthermore, electromyography (EMG) amplitude following 14 days of unilateral lower limb suspension (ULLS) decreased in the immobilised limb along with peak torque, while limb mass remained unchanged (Deschenes *et al.*, 2002), all of which highlight potential neural dysregulation. The extent of disuse atrophy is also muscle dependent which has led to the descriptors of 'atrophy resistant' and 'atrophy susceptible' muscles (Bass *et al.*, 2021). A recent systematic review consolidated previous work to date (Campbell *et al.*, 2019), and of the 40 studies included, 20 immobilised the knee, preventing use of one of the most functionally relevant muscle groups, i.e., the quadriceps. Furthermore, just 20 studies investigated neural factors (i.e., using surface EMG), yet adaptations of individual MU characteristics, particularly at the NMJ, remain largely unexplored.

The purpose of the study was to quantify neuromuscular changes by studying individual MU features in the immobilised and non-immobilised limbs by utilising intramuscular EMG (iEMG) to sample individual MUs from the VL pre and post 15-days of immobilisation. We hypothesised that, coinciding with a reduction in muscle mass and strength, NMJ transmission instability would increase, and MU firing rate would decrease in the immobilised leg, with no change to the non-immobilised limb.

Methods

Ethical approval

This study was approved by the University of Nottingham Faculty of Medicine and Health Sciences Research Ethics Committee (103-1809) and conformed with the Declaration of Helsinki. It was registered online at clinicaltrials.gov (NCT04199923). Participants were recruited locally from the community via advertisement posters in print and on research group social media pages. Ten healthy, young male participants were recruited to take part in the study. After providing written informed consent to participate in the study, potential participants were screened for eligibility against pre-determined exclusion criteria, including active cardiovascular, cerebrovascular, respiratory, renal, or metabolic disease, active malignancy, musculoskeletal or neurological disorders. Once eligibility was confirmed, participants were invited to the laboratory for baseline testing, as described below.

Muscle ultrasound

Vastus lateralis (VL) cross sectional area scans (CSA) were taken at the mid-belly of the muscle. This was located by measuring the length from the midline of the patella to the greater trochanter and taking the middle value of that line. Following this, a narrow ultrasound probe (LA523 probe and MyLab™50 scanner, Esaote, Genoa, Italy) was used to find the medial and proximal borders of the muscle where the aponeurosis of the VL intersected with the *vastus intermedius*. Three axial plane images were collected following this line from both legs and subsequently analysed using ImageJ (Laboratory of Optical and Communication, University of Wisconsin-Madison, WI, USA) to quantify CSA (Scott *et al.*, 2017).

Lower limb power

Explosive unilateral lower limb power was assessed using the Nottingham Power Rig (University of Nottingham; (Bassey & Short, 1990)). For this, participants were seated on the purpose-built rig with their knee at 90° when the foot was on the plate. The rig is designed to isolate power production from the lower limb. Following a 3 s countdown, participants were instructed to perform an explosive push. The power exerted was displayed digitally and the highest of three attempts recorded.

Maximal voluntary isometric contraction

Participants were seated in a custom-built isometric dynamometer with their knee joint angle fixed at 90° while the hip joint angle was at 110°. The ankle was secured in place to a plate connected to a force transducer. Three moderate intensity warm-up contractions were carried out with visual feedback of force traces on a screen in front of the participants. Using a waist belt to prevent hip lifting

and facilitate isolation of the knee extensors, participants were verbally encouraged to perform an isometric knee extension at maximal capacity.

Vastus lateralis motor point identification

Using low intensity percutaneous electrical stimulation (400V, pulse width 50 µS, current ~10 mA; delivered via a Digitimer DS7A, Welwyn Garden City, UK), the surface of the VL was explored to find the point producing the greatest visible twitch with the lowest current, i.e., the motor point (Piasecki *et al.*, 2016*a*).

Force and electromyography recording

Surface electromyography was arranged in a bipolar configuration. The recording electrode was placed over the identified motor point and the reference electrode over the patellar tendon (disposable self-adhering Ag-AgCl electrodes; 95 mm^2; Ambu Neuroline, Baltorpbakken, Ballerup, Denmark). A ground electrode was placed just above the reference electrode on the patella (Ambu Neuroline Ground). EMG signals were digitised (CED Micro 1401; Cambridge Electronic Design, Cambridge, UK) and Spike2 (version 9.00a, CED) software was used to provide a real-time display of the signal on screen. Peak twitch force was calculated using percutaneous electrical stimulation (Digitimer, UK), and the maximal M-wave was measured with surface electromyography at the motor point. A stimulating pen was placed over the femoral nerve in the inguinal fold and stimulation intensity (400V, pulse width 50 µS, current typically 70-110 mA) was increased until the M-wave amplitude displayed in Spike2 plateaued. The peak force generated corresponding to the maximal M-wave was recorded, and all force signals were recorded at 100 Hz. Force steadiness was assessed during the sustained voluntary contractions as the coefficient of variation of the force deviation from the target line, averaged at each contraction intensity. The first two passes of the target (<1s) were excluded from the calculation to avoid corrective actions when reaching the target line.

Intramuscular electromyography

A concentric needle electrode (Ambu Neuroline model 740 25-45/25, Ambu, UK) was inserted at the *vastus lateralis* motor point. The recorded iEMG signals were sampled at 50 kHz and bandpass filtered from 10 Hz to 10 kHz (1902 amplifier, CED). A real-time display was observed using Spike2 (CED) and data were stored offline for analysis. Once the needle was inserted, contractions were carried out at 10% and 25% of the participants MVC following a visual target line. Six contractions were recorded at each intensity, with the needle electrode position altered between each to sample a broader range of MUPs (Jones *et al.*, 2021). From the original position, the needle electrode was slightly withdrawn, and the bevel rotated 180° at each depth and positioned to maximise signal to noise ratio. These voluntary contractions were held for 12 s with a 10-20 s rest in between each contraction.

152 EMG analysis

153 Decomposition-based quantitative electromyography (DQEMG) software was used to process raw
154 EMG data. This involved the detection of MUPs and extraction of MUP trains (MUPTs) from individual
155 MUs generated during sustained iEMG signals recorded during voluntary contractions at set
156 intensities. MUPTs were excluded if they contained MUPs from multiple MUs or fewer than 40 MUPs.
157 MUP templates were visually inspected to ensure markers were placed correctly to start, end, positive
158 and negative peaks of the waveforms. MUP area was defined as the integral of the absolute value of
159 MUP values recorded between start and end markers multiplied by the sampling time interval in
160 µV/ms (Piasecki *et al.*, 2021*b*). MUP amplitude was determined as the measurement from the maximal
161 positive and negative peaks of the waveform (Guo *et al.*, 2022). MUP complexity, measured as the
162 number of turns, was defined as the number of significant slope direction changes within the duration
163 of the MUP of a height >20 µV. A near fibre MUP (NF-MUP) was obtained from each MUP by estimating
164 the slopes of each MUP (Piasecki *et al.*, 2021*b*) and NMJ transmission instability, measured as near-
165 NF-MUP jiggle, was determined as the normalised means of median consecutive amplitude
166 differences (Piasecki *et al.*, 2021*b*). MU firing rate (MU FR) was recorded as the rate of occurrence per
167 second of MUPs within a MUPT in Hz, and MU FR variability was determined as the coefficient of
168 variation of the inter-discharge interval.

169 Immobilisation procedure

170 For the 15 days of immobilisation, a unilateral lower-limb suspension (ULLS) model was used. The knee
171 joint was fixed at 75° flexion using a hinged leg brace (Knee Post op Cool, Össur, Iceland) with the
172 ankle joint fixed using an air-boot (Rebound Air Walker, Össur), ensuring that the immobilised leg was
173 not able to bear any weight. Crutches were provided and adjusted according to the height of the
174 participant, and training on their effective use was provided. The brace and boot remained in place at
175 all times, including sleeping and bathing, with tamper tags attached to each to monitor intervention
176 adherence.

177 Follow-up testing

178 Following 15 days of ULLS, participants were invited back to the laboratory for post-immobilisation
179 testing. All procedures carried out in the baseline testing visit were repeated in both legs. In addition
180 to measuring FS and iEMG at 25% of post-immobilisation MVC (i.e., relative force, referred to as
181 follow-up force), iEMG was also performed at 25% of pre-immobilisation MVC (i.e., absolute force,
182 referred to as baseline force) to compare FS and MU characteristics normalised to pre and post disuse-
183 induced strength loss.

184 Statistical analysis

Statistical analysis of MVC and ultrasound CSA was carried out using GraphPad Prism version 9.1.0 (GraphPad Software, CA, USA) using repeated measures 2-way analysis of variance with Šidak's post-hoc analysis. Multi-level mixed effect linear regression models were used to analyse MU parameters, in StataSE (v16.0, StataCorp LLC, TX, USA). For both analyses, two within-subject factors were assessed: time (pre and post) and leg (immobilised and control). Where no leg x time interactions were present, separate models were performed to assess effects of time in individual limbs. Additional exploratory analyses were performed to investigate relationships between iEMG variables and key physiological outcome variables – muscle strength (MVC) and size (CSA) using R (Version 4.2.0, (https://cran.r-project.org/) implemented using R studio. Firstly, correlative analysis was assessed with Pearson's product moment correlation coefficient and visualised using corrplot (https://cran.r-project.org/web/packages/corrplot) to determine any strong relationships between variables. Cluster analysis and principal component analysis for variables were performed using the ClustOfVar (https://cran.r-project.org/web/packages/ClustOfVar) and factoextra (https://cran.r-project.org/web/packages/factoextra) packages respectively, to determine which variables strongly clustered and related to others. Finally, using a subset of these best clustering variables, multivariate linear regression was performed to determine which clustered variables best predict changes in MVC and CSA. Significance was assumed if $p<0.05$.

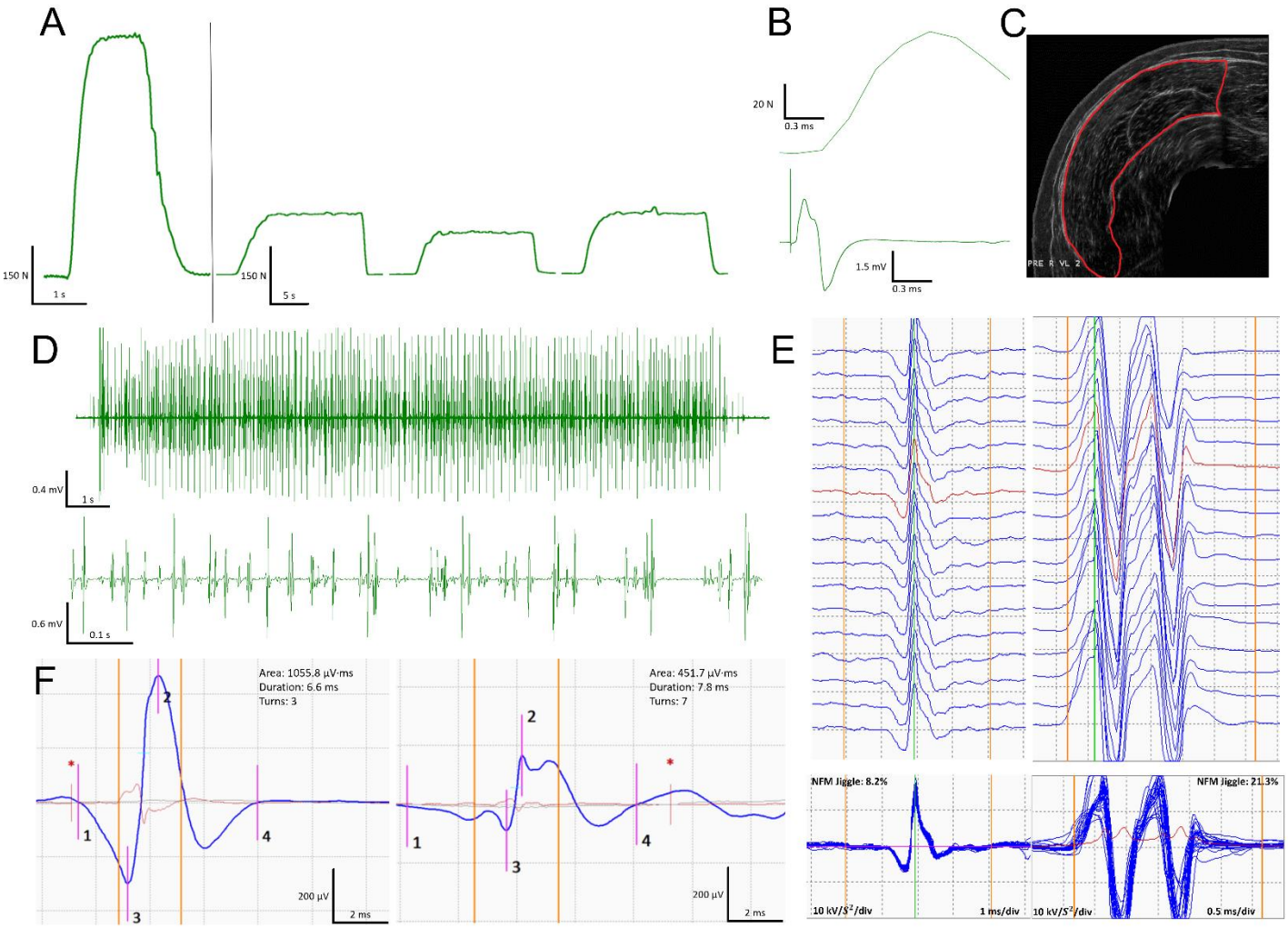

Figure 1: (A) *Knee extensor force traces (left to right) from a maximal voluntary isometric contraction (MVC), 25% of MVC contraction pre 15-day unilateral limb immobilisation, 25% contraction post-immobilisation relative to follow-up MVC, and 25% contraction post-immobilisation relative to baseline MVC.* ***(B)*** *Peak twitch force recording showing force trace (upper) and corresponding surface electromyography EMG recorded M-wave (lower) from a maximal stimulation of the femoral nerve.* ***(C)*** *An example ultrasound scan of the m. vastus lateralis used to calculate cross-sectional area.* ***(D)*** *Example intramuscular EMG (iEMG) trace recorded during a 12 second voluntary isometric contraction (upper) and magnified (lower) with visible motor unit potentials (MUP).* ***(E)*** *Example raster plots (upper) and corresponding shimmer plots (lower) from near-fibre MUPs (NF-MUP) before (left) and after (right) immobilisation recorded during active contractions.* ***(F)*** *Example MUPs recorded before (left) and after (right) immobilisation. N; newtons, s; seconds, ms; milliseconds, V; volts, µV; microvolts, kV/s^2; kilovolts per second squared, µV·ms; microvolts per millisecond.*

Results

Participant Characteristics

Ten male participants took part in this study. Characteristics are shown in table 1.

Table 1: *Descriptive characteristics of participants showing mean and standard deviation (SD)*

N = 10	Mean (SD)
Age (years)	23.68 (3.36)
Height (cm)	181.56 (6.69)
Weight (kg)	79.37 (9.70)
BMI (kg/m^2)	24.02 (2.10)

Muscle Size and Function

There was a significant leg x time interaction in VL CSA ($p<0.001$, n=9), which decreased in the immobilised leg after 15 days (-15%, $p<0.001$) and remained unchanged in the control leg (p=0.78, fig. 2A). Similarly, there was a significant leg x time interaction of knee extensor MVC ($p<0.01$), which decreased in the immobilised leg (-31%, $p<0.001$) while no change was seen in the control leg (p=0.498, fig. 2B). Peak twitch force (n=7) showed no significant leg x time interaction (p=0.0582). No change was seen in either the immobilised leg (p=0.130) or the control leg (p=0.410) following the immobilisation period (fig. 2C). Unilateral lower limb power output (n=9) presented a significant leg x time interaction (p=0.0172), which reduced significantly in the immobilised limb (-26%, p=0.0037) while remaining unchanged in the control leg (p=0.939, fig. 2D). Force steadiness (FS) at 10% MVC presented a significant leg x time interaction (p=0.0201, fig. 2E), with non-significant changes in the immobilised limb (-14%, p=0.065) and the control (+4%, p=0.278). No interaction was present in FS at 25% MVC (p=0.255), with no changes observed when exploring limbs individually (immobilised: p=0.999, control: p=0.221, fig. 2E).

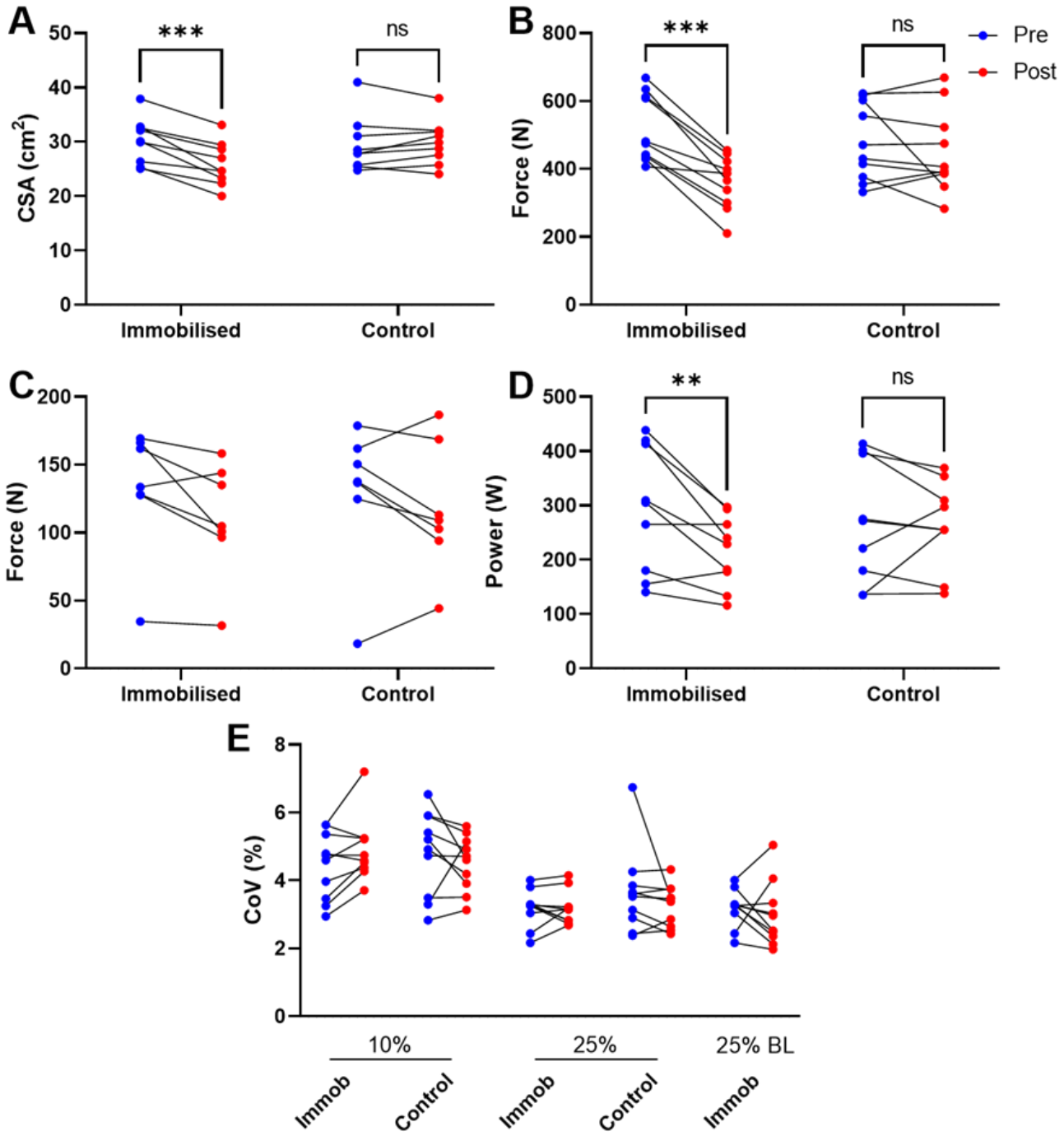

234 ***Figure 2:*** *All figures show data before and after 15-day unilateral lower limb suspension in the*
235 *immobilised and control legs.* ***A:*** *Vastus lateralis cross-sectional area (cm²) measured by ultrasound*
236 *(n=9).* ***B:*** *Knee extensor maximal voluntary isometric contraction force (N).* ***C:*** *Peak twitch force (N, n=7)*
237 *measured from maximal involuntary contraction elicited by femoral nerve stimulation.* ***D:*** *Unilateral*
238 *lower limb power measured using the Nottingham Power Rig.* ***E****: Knee extensor force steadiness*
239 *measured during contractions at 10 and 25% relative to both follow-up and baseline maximal*
240 *voluntary isometric contraction. Coefficient of variation shown as average deviation from target line*
241 *(individual mean values shown pre to post in immobilised and control legs at each contraction*

*intensity). For all parameters, analysis performed via repeated measures 2-way analysis of variance with Šidak's post-hoc analysis. ** = p<0.01, *** = p<0.001.*

Neuromuscular Parameters

Contractions at 25% MVC were carried out relative to follow-up MVC as well as baseline MVC. Mean values for each parameter are shown in Figures 4 and 5. MUP area at 10% MVC presented no significant leg x time interaction (p=0.091, fig. 3A). Following post-hoc analysis, a reduction was seen in the immobilised leg (p<0.001) while no change was seen in the control leg (p=0.443). At 25% follow-up MVC, a significant interaction was seen (p=0.028, fig. 4A), reflected by a reduction in the immobilised leg (p<0.001) but no change in the control (p=0.717). At 25% baseline MVC, a significant reduction in MUP area (p<0.001) was present. For MUP amplitude at 10% MVC, there was no significant leg x time interaction (p=0.106, fig. 2B). In the immobilised leg a significant reduction was present (p<0.001) with no change in the control leg (p=0.283). At 25% follow-up MVC, amplitude presented a significant leg x time interaction (p=0.046, fig. 3B), with a reduction in the immobilised leg (p=0.007) but no change in the control (p=0.881). At 25% baseline MVC MUP amplitude was also significantly reduced (p=0.006).

MUP complexity, defined as the number of turns, presented no significant leg x time interaction at 10% MVC (p=0.660, fig. 3C), with post-hoc analysis showing an increase in the immobilised leg (p=0.022), but no change in the control (p=0.204). At 25% follow-up MVC, complexity had a significant leg x time interaction (p=0.007, fig. 4C). An increase was seen in the immobilised leg (p=0.001) but no change was seen in the control (p=0.600). At 25% baseline MVC MUP complexity did not change significantly (p=0.073). At 10% MVC, NMJ transmission instability showed no leg x time interaction (p=0.191, fig. 3D), with no change in either the immobilised (p=0.152) or control (p=0.759) legs. Similarly at 25% follow-up MVC, no leg x time interaction was seen (p=0.966, fig. 4D). However, a significant increase was seen in the immobilised leg (p=0.008) but no change in the control (p=0.164). At 25% baseline MVC, NMJ transmission instability was also increased (p=0.024).

Motor unit FR presented a significant leg x time interaction at 10% MVC (p=0.022, fig. 3E), with a reduction in the immobilised leg (p<0.001) but no change in the control (p=0.848). At 25% follow-up MVC, an interaction was also observed (p<0.001, fig. 4E), again showing a reduction in the immobilised leg (p<0.001) but no change in the control (p=0.563). At 25% baseline MVC, firing rate was also decreased (p<0.001). Finally, firing rate variability presented no leg x time interaction at 10% (p=0.070, fig. 3F), with a reduction in the immobilised leg (p=0.001) and no change in the control (p=0.668). At 25% follow-up MVC, a significant interaction was seen (p=0.001, fig. 4F), with a reduction in the

immobilised leg (p<0.001) and no change in the control (p=0.574). However, at 25% baseline MVC firing rate variability remained unchanged (p=0.193).

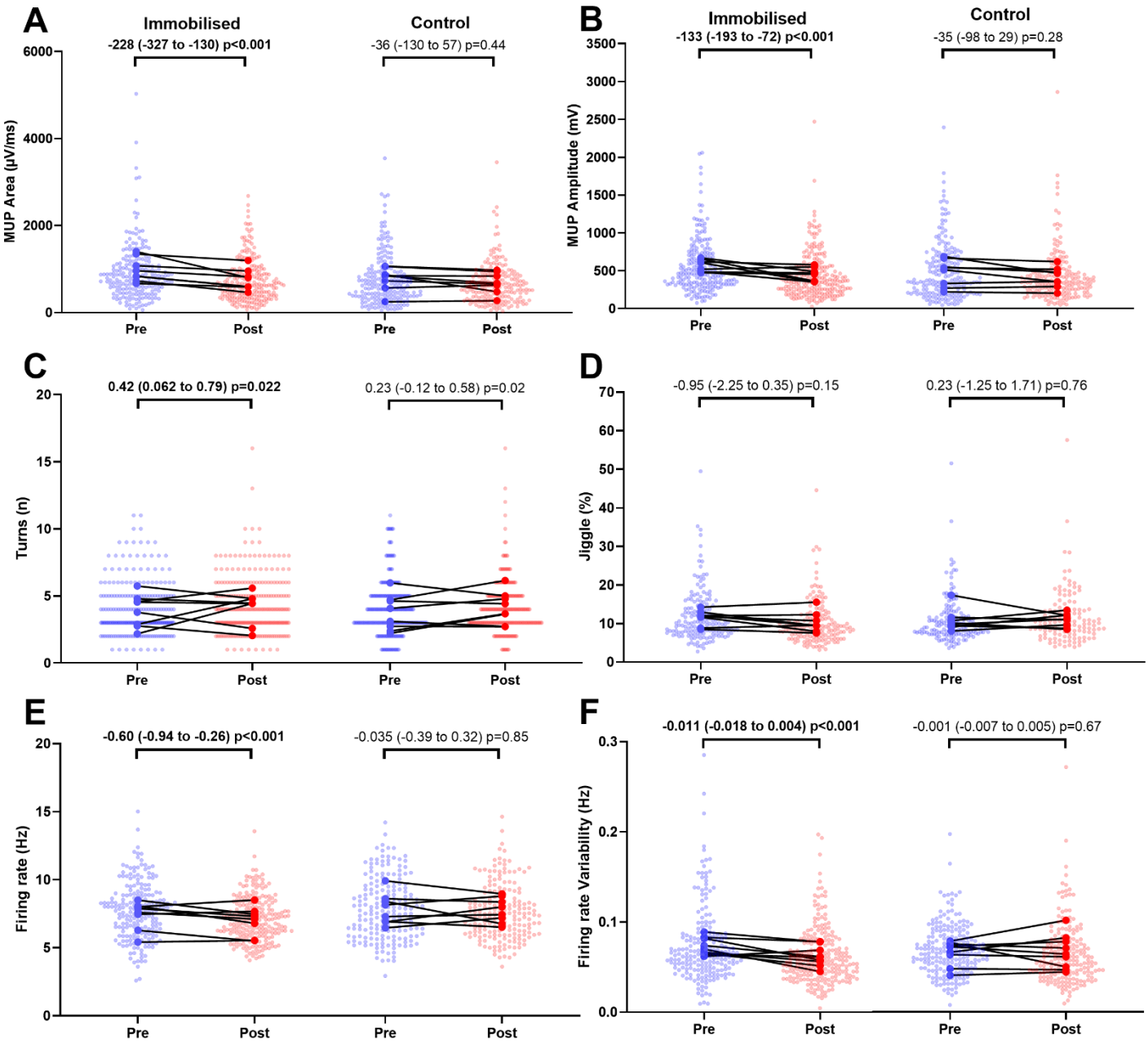

Figure 3: *Motor unit potential parameters and MU discharge characteristics of motor units sampled during contractions performed at 10% maximal voluntary force before and after 15-day unilateral leg immobilisation in both immobilised and control legs. Data show mean values and pooled MUs with comparison bars showing β coefficient and 95% CI from multi-level mixed effects models. N = 9.*

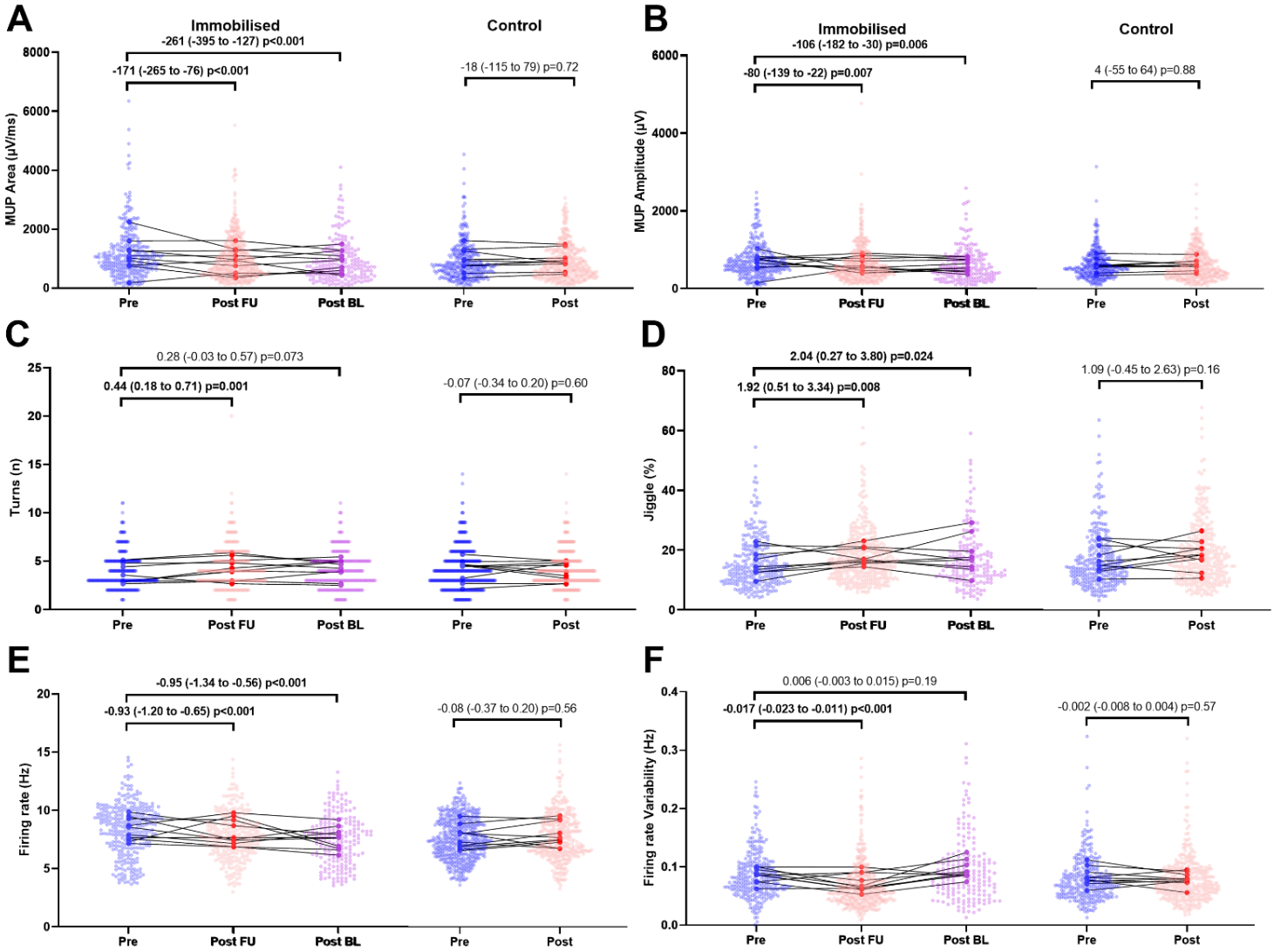

Figure 4: *Mean values of motor unit potential parameters and MU discharge characteristics of motor units sampled during contractions performed at 25% maximal voluntary force before and after 15-day unilateral leg immobilisation in both immobilised and control legs. Values in the immobilised leg post-immobilisation are relative to follow-up MVC (column 2) and relative to baseline MVC (column 3) due to reduced MVC following immobilisation. Data show mean values and pooled MUs with comparison bars showing β coefficient and 95% CI from multi-level mixed effects models.*

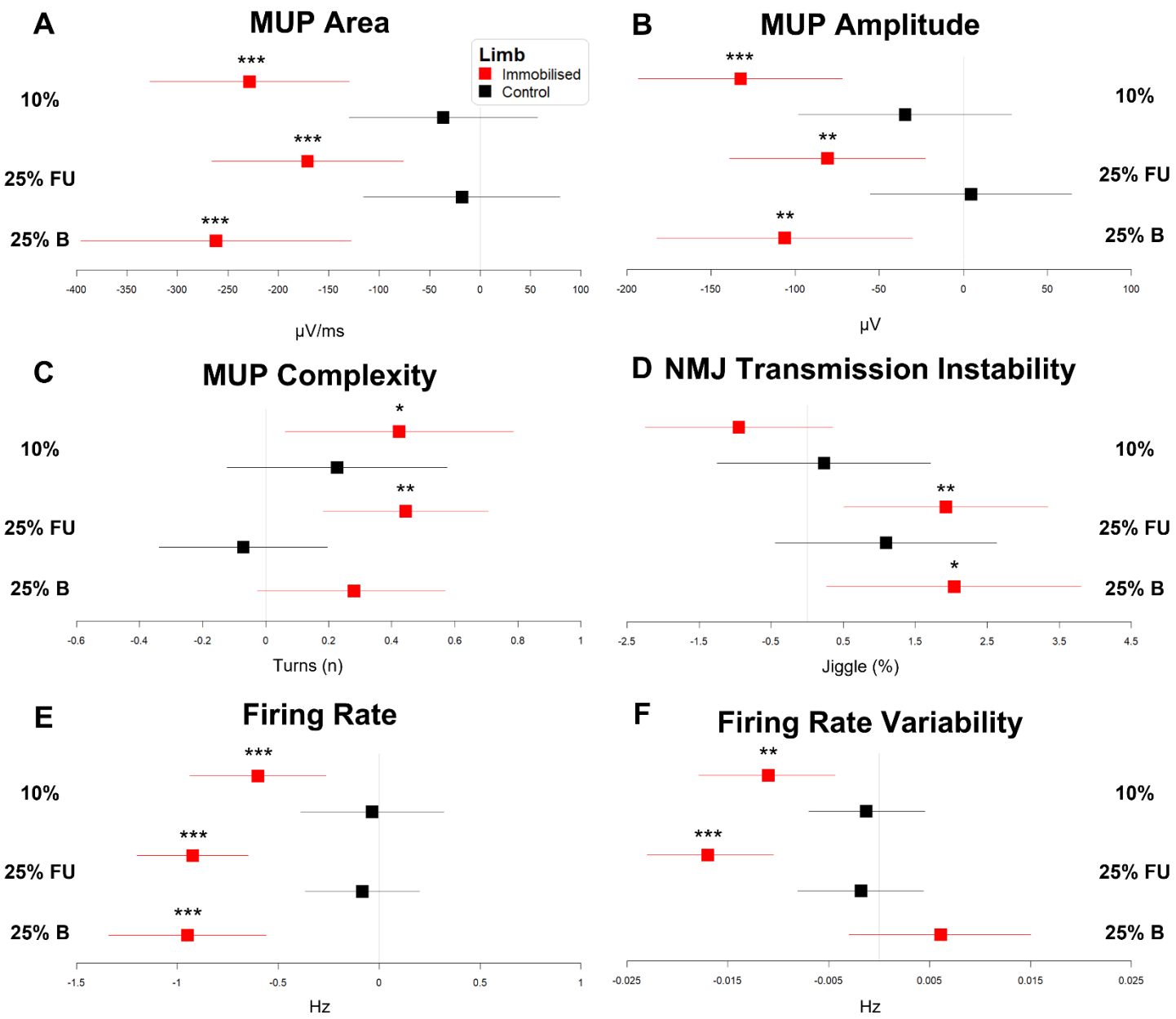

Figure 5: *Forest plots summarising data from motor unit parameters measured from the vastus lateralis during 10% MVC, and 25% normalised to follow-up (FU) and baseline (B) MVC. Plots display beta coefficient and 95% confidence intervals from multi-level mixed linear regression models. * = p<0.05, ** = p<0.01, *** = p<0.001.*

In exploratory analyses, to investigate potential relationships between neuromuscular parameters and muscle strength and size, correlation analysis was performed on mean differences between parameters assessed at 25% pre and 25% post MVC (fig. 6). Strong correlations were observed between MUP area and amplitude (r^2=0.846, p=0.0003) and between NF-MUP jiggle and MVC (r^2=0.792, p=0.0082). To more accurately reflect relationships between these variables, clustering of these variables was performed using the hierarchical clustering algorithm provided in ClustOfVar and further visualised using principal component analysis score plots (PCA, fig. 7). The key cluster of interest consisted of MVC, CSA, NF-MUP jiggle, FR and FR variability. To test whether the neuromuscular parameters in this cluster had any influence on the changes observed in muscle strength and size, the values were first normalised to the same dynamic range before multivariate linear regression was performed. There were no significant relationships for either MVC or CSA with NF-MUP jiggle (p=0.245 and p=0.124 respectively), FR variability (p=0.0907 and p=0.0793) and FR (p=0.105 and p=0.144). However, the strongest predictor of both change in MVC and CSA due to immobilisation was FR Variability.

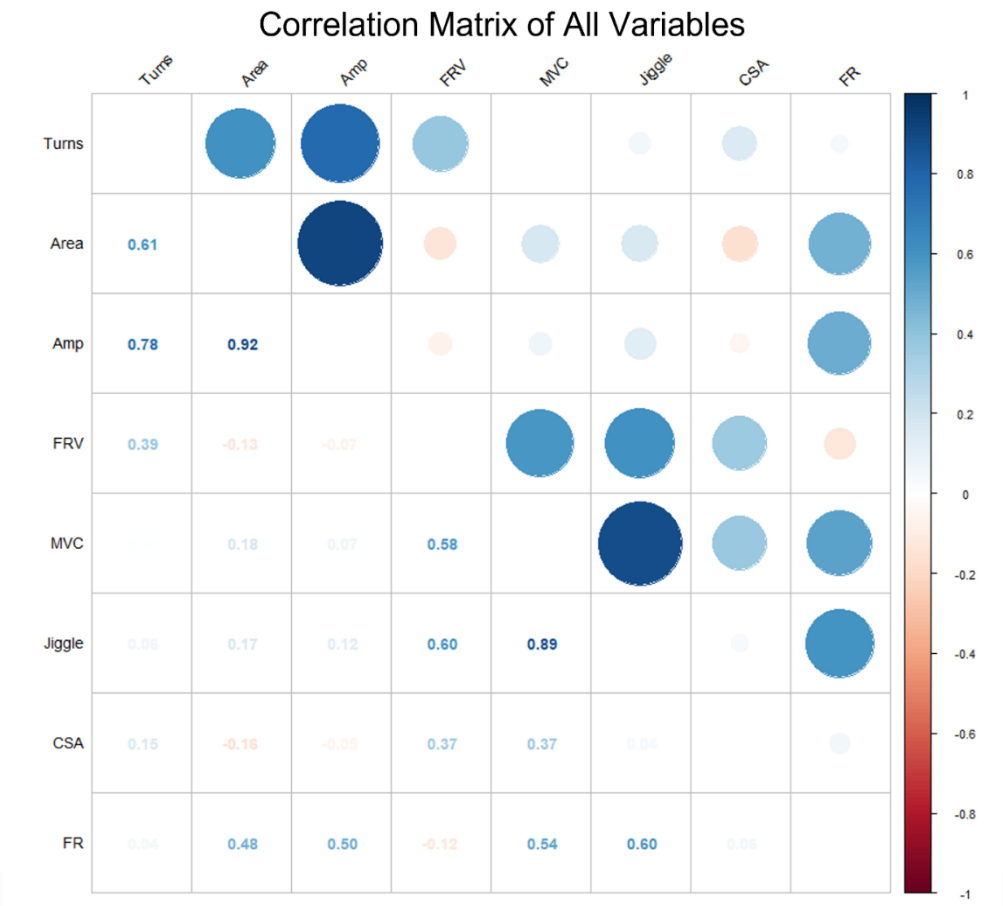

Figure 6: *Correlation matrix of relationships between eight variables measured in this study. Amp; amplitude, FRV; firing rate variability, MVC; maximal voluntary contraction, CSA; cross-sectional area, FR; firing rate.*

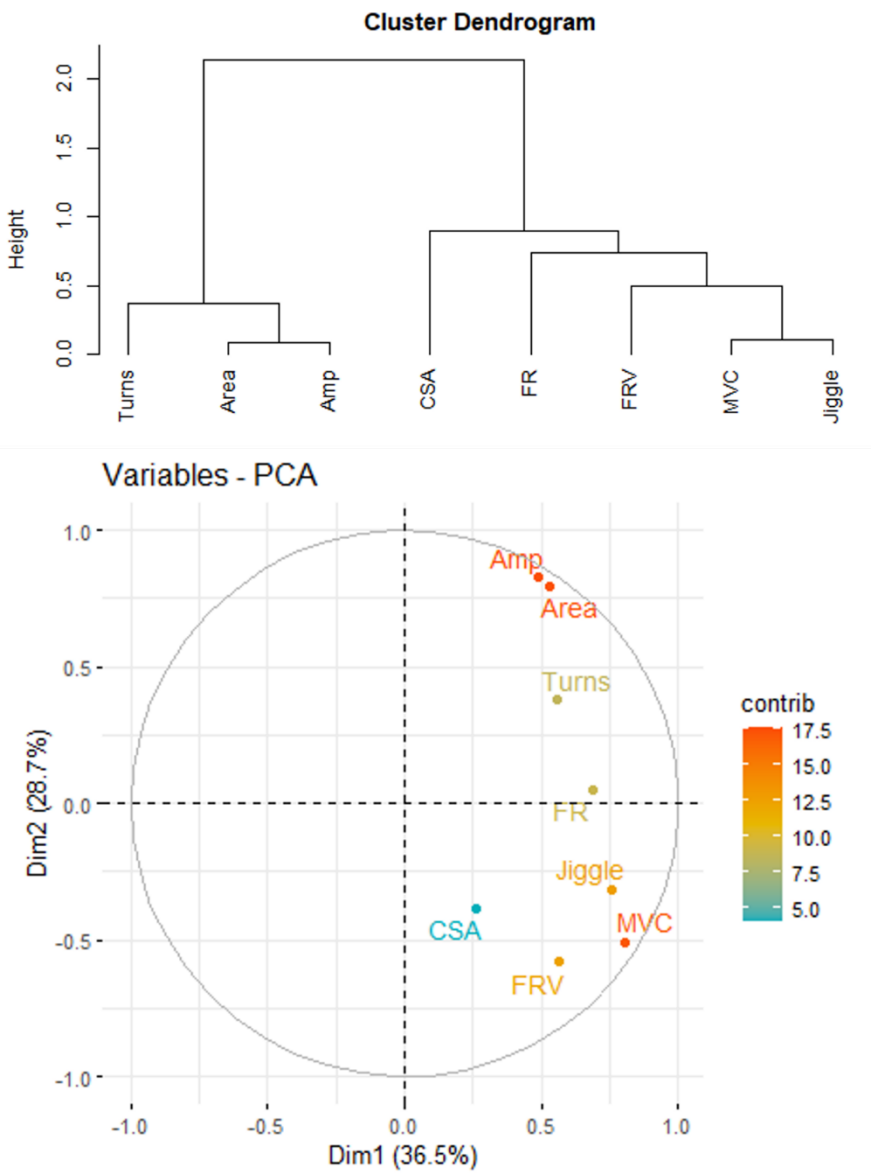

Figure 7: *Cluster tree plot (upper) and accompanying principal component analysis plot (lower) to illustrate relationships between variables within the first two dimensions of variance between variables. Amp; amplitude, FRV; firing rate variability, MVC; maximal voluntary contraction, CSA; cross-sectional area, FR; firing rate, Dim; dimension.*

337 **Discussion**

338 This study has characterised the adaptations of individual VL MUs following 15 days unilateral lower-
339 limb immobilisation, in immobilised and non-immobilised limbs. Our findings reveal a number of
340 adaptations that are unique to the immobilised limb only, with the non-immobilised limb largely
341 unaffected. Muscle of the immobilised leg became smaller and weaker, and individual MUPs became
342 smaller and more complex. Motor units of the immobilised leg had greater NMJ transmission
343 instability, with reduced FR. Notably, the majority of these decrements were still apparent when force
344 levels were normalised to that achieved prior to immobilisation, highlighting impaired neural input to
345 muscle as a prominent contributor to the observed reduction in muscle function.

346 The observed decline in muscle strength (-31%) in the immobilised limb exceeded the decline in
347 muscle CSA (-15%), and this discordant finding supports several other studies employing a ULLS model;
348 14-day unilateral knee immobilisation with an ~5% decrease in quadriceps CSA and a ~25% decline in
349 isometric strength (Glover *et al.*, 2008), and following 14 days of limb cast immobilisation, an ~8.5%
350 decline in quadriceps CSA was observed alongside a ~23% decline in muscle strength (Wall *et al.*,
351 2014). Unilateral power output was reduced in the immobilised limb only. Bed rest studies have
352 collectively shown a reduction in muscle performance of ~3% per day, although this reduction in bed
353 rest was seen to stabilise between day 5 and day 14, suggesting a sharp initial reduction (Di Girolamo
354 *et al.*, 2021) which may have also occurred in the present study. Furthermore, the control limb
355 remained unaffected in terms of functional loss and does not support the concept of a negative cross-
356 over effect on measures of neuromuscular function. Peak twitch force was unaltered when assessed
357 with an involuntary contraction elicited from a single pulse to the femoral nerve, and likely reflects
358 the lack of sensitivity of this method. Similarly, force steadiness was not affected by immobilisation at
359 low or mid-range contraction intensities and indicates a preservation of basic motor control following
360 disuse.

361 MUP size (area and amplitude) is reflective of the depolarisation of all fibres within a single MU, within
362 the detection area of an indwelling electrode and is proportional to the size and number of fibres
363 contributing to it. Area and amplitude were significantly decreased post-intervention at both 10 and
364 25% MVC contraction intensities in the immobilised leg only, and were unsurprisingly highly
365 correlated. While greater MUP size increase is commonly observed in aged muscle reflecting MU
366 remodelling and reinnervation of denervated muscle fibres (Jones *et al.*, 2022), smaller MUPs
367 differentiated sarcopenic from non-sarcopenic older men in this muscle group (Piasecki *et al.*, 2018).
368 The reduction observed here may indicate partial denervation of MU fibres as a result of disuse, or, it
369 may reflect extensive fibre atrophy across MU fibres sampled at these contraction levels. MUP size
370 reduction has also been observed in dystrophinopathies (Zalewska *et al.*, 2013), where amplitude in

371 the biceps brachii was significantly below reference values in patients with Duchene and Becker
372 muscular dystrophies (Zalewska *et al.*, 2004). All markers of MUP size increase with increasing
373 contraction level, reflecting the recruitment of additional, larger MUs (Guo *et al.*, 2022), and the
374 decreases observed in the immobilised leg were apparent at 25% follow-up *and* baseline MVC. This
375 finding highlights that reduction of force post-immobilisation cannot explain the decline in MUP size
376 and is more likely related to a reduction in muscle fibre size and/or partial denervation/reinnervation
377 of fibres.

378 Similar to MUP size, MUP complexity, defined as the number of MUP turns, was significantly greater
379 in the immobilised leg only following the intervention, at both contraction intensities which is
380 indicative of a greater temporal electrophysiological dispersion between individual fibres of the same
381 MU (Stålberg & Sonoo, 1994; Piasecki *et al.*, 2021*b*) as a result of an increased difference in conduction
382 times along axonal branches and/or MU fibres. Increased MUP complexity has been observed in
383 various myopathies which are suggestive of increased fibre diameter variability and also in
384 neuropathies, expressing 75% greater turns than the control cohort, which is thought to be a product
385 of the reinnervation and longer conduction times along axonal sprouts (Stewart *et al.*, 1989). This has
386 been reinforced specifically in myopathic conditions, as data from primarily the biceps brachii along
387 with recordings of the vastus lateralis and gastrocnemius showed an 82% increase in polyphasic MUPs
388 (Uncini *et al.*, 1990). While much less severe, the changes seen following immobilisation may also
389 follow a common pathway linked to denervation and reinnervation. This may suggest that some
390 reinnervation has occurred following immobilisation, or alternatively that selective reduction in
391 muscle fibre diameter has taken place, affecting MU fibres unequally resulting in more variable muscle
392 fibre action potential propagation. Although needle insertions around the muscle motor point help to
393 minimise the effects of variable muscle fibre conduction times and enable greater focus on axonal
394 branch conduction variability, the specific motor endplate location remains an unknown *in vivo* and
395 these effects cannot be completely excluded.

396 NMJ transmission instability, reported as NF MUP jiggle, was also significantly greater following the
397 intervention in the immobilised leg only. NMJ structural stability was reported to decrease following
398 10-day bed rest, inferred following an increase in C-terminal agrin fragment (CAF) observed in serum
399 at day 10 (Monti *et al.*, 2021). It is suggested that CAF presence may be indicative of a dysregulation
400 at the NMJ, reducing myoelectrical transmission reliability and therefore contractile activity in the
401 muscle. However, it is not clear if this evidence represents active NMJ transmission as it is not directly
402 measured during muscle contraction. Nevertheless, the *in vivo* methods applied here support the
403 finding that disuse atrophy is accompanied by increased instability of transmission at the NMJ,
404 possibly reflecting a partial denervation/reinnervation process. This process has been reported in

healthy ageing (Hourigan *et al.*, 2015; Piasecki *et al.*, 2016*b*, 2021*a*) and diabetic neuropathy (Allen *et al.*, 2015) corresponding with larger MUPs. Abnormally high NF MUP jiggle values have also been reported in the tibialis anterior of patients with chronic inflammatory demyelinating polyneuropathy (Gilmore *et al.*, 2017) where an average increase of 90% compared to healthy controls was seen. This was associated with increased MUP area and complexity, also attributed to an incomplete reinnervation process. Herein, NMJ transmission instability was also greater when contraction intensity was normalised to baseline MVC following immobilisation, indicating that NMJ dysregulation is prevalent through a wider pool of motor units responsible for a broader range of contraction force.

The reduced MU FR reported here following immobilisation and loss of strength, may initially be explained by the lower absolute forces produced. However, this suppression of firing rate was also apparent at contractions normalised to baseline strength and clearly highlights it as a contributor to functional decrements. Ionotropic synaptic inputs and neuromodulation control the excitability of motoneurons, the latter of which is largely mediated by the amplitude of persistent inward currents (PICs) which act to amplify synaptic input and are proportional to the level of localised monoamine release (Heckman *et al.*, 2008). Although difficult to quantify *in vivo*, it is possible monoamine levels decrease in response to reduced activity, yet it is unclear how this would influence the immobilised limb only. PIC amplitudes are also sensitive to inhibition (Hyngstrom *et al.*, 2007; Mesquita *et al.*, 2022), and recent RNAseq data highlight increased ligand-receptor interactions between muscle and dorsal root ganglion neurons following disuse, suggestive of an increased nociceptor sensitivity and susceptibility to pain (McFarland *et al.*, 2022). As such, it is possible increased inhibition occurred in the immobilised limb only and suppressed PIC amplitudes and MU FR, similar to that believed to explain decreased FR following knee joint trauma (Nuccio *et al.*, 2021). Reduction in firing rate variability at 10% MVC and 25% follow-up MVC may be viewed as a positive adaptation, however it more likely reflects the reduction in firing rate at lower absolute forces (Guo *et al.*, 2022) as it was not apparent when force was normalised to baseline MVC.

Additional analysis into factors potentially related to the reduction in force and changes in neuromuscular parameters found a clustering of NMJ transmission instability, MU FR and FR variability with MVC and CSA. Following multivariate simple linear regression, no significant relationships were observed between either muscle size or strength with those neuromuscular parameters. This suggests that, in these data, no single variable fully explained the decline in muscle strength and size.

Since the average length of hospital stay in the United Kingdom as of 2018/19 was 4.5 days (Ewbank *et al.*, 2020), future work in disuse should focus on the impact of such a short time frame on the neural

437 input to muscle. Understanding these changes will provide a mechanistic basis on which to optimise
438 rehabilitation protocols to counteract reduced muscle function.

439 Limitations

440 A limitation to this study is that the contraction intensities at which motor units were sampled are of
441 the low to mid-level and reveal nothing of adaptation to later recruited MUs. Knee extensor
442 movements are not uniquely controlled by the VL, and although it may be a useful proxy for total
443 quadriceps, we cannot rule out greater decrements in other muscles of this group. The current data
444 are available in males only, and although we have highlighted similar differences across contractions
445 in young males and females (Guo *et al.*, 2022), there are sex-based differences in MU FR at normalised
446 contraction levels which may respond differently to this intervention.

447 Conclusion

448 These results support previous findings that unilateral short-term immobilisation of just 15 days leads
449 to a decline in muscle strength unmatched by that in muscle size. Importantly, the current data
450 highlight that this disconnect is explained by central and peripheral adaptations to neural input to
451 muscle, evidenced by suppressed MU FR and increased instability of transmission at the NMJ, and
452 identifies interventional targets for cases of muscle disuse.

453

454 References

455 Allen MD, Stashuk DW, Kimpinski K, Doherty TJ, Hourigan ML & Rice CL (2015). Increased
456 neuromuscular transmission instability and motor unit remodelling with diabetic neuropathy as
457 assessed using novel near fibre motor unit potential parameters. *Clin Neurophysiol* **126,** 794–
458 802. DOI: 10.1016/j.clinph.2014.07.018.

459 Bass JJ, Hardy EJO, Inns TB, Wilkinson DJ, Piasecki M, Morris RH, Spicer A, Sale C, Smith K, Atherton
460 PJ & Phillips BE (2021). Atrophy Resistant vs. Atrophy Susceptible Skeletal Muscles: "aRaS" as a
461 Novel Experimental Paradigm to Study the Mechanisms of Human Disuse Atrophy. *Front*
462 *Physiol* **12,** 1–11. DOI: 10.3389/fphys.2021.653060.

463 Bassey EJ & Short AH (1990). A new method for measuring power output in a single leg extension:
464 feasibility, reliability and validity. *Eur J Appl Physiol Occup Physiol* **60,** 385–390. DOI:
465 10.1007/BF00713504.

466 Campbell M, Varley-Campbell J, Fulford J, Taylor B, Mileva KN & Bowtell JL (2019). Effect of
467 Immobilisation on Neuromuscular Function In Vivo in Humans: A Systematic Review. *Sport Med*
468 **49,** 931–950. DOI: 10.1007/s40279-019-01088-8.

469 Castro MJ, Apple DF, Rogers S & Dudley GA (1999). Influence of complete spinal cord injury on
470 skeletal muscle mechanics within the first 6 months of injury. *Eur J Appl Physiol Occup Physiol*
471 **81,** 128–131. DOI: 10.1007/PL00013785.

472 Deschenes MR, Giles JA, McCoy RW, Volek JS, Gomez AL & Kraemer WJ (2002). Neural factors
473 account for strength decrements observed after short-term muscle unloading. *Am J Physiol -*
474 *Regul Integr Comp Physiol* **282,** 578–583. DOI: 10.1152/ajpregu.00386.2001.

475 Duchateau J & Hainaut K (1990). Effects of immobilization on contractile properties, recruitment and
476 firing rates of human motor units. *J Physiol* **422,** 55–65. DOI: 10.1113/jphysiol.1990.sp017972.

477 Ewbank L, Thomson J, Helen M & Anandaciva S (2020). NHS hospital bed numbers: past, present,
478 future. *King's Fund*1–19. . Available at: https://www.kingsfund.org.uk/publications/nhs-
479 hospital-bed-numbers [Accessed October 7, 2021].

480 Gilmore KJ, Allen MD, Doherty TJ, Kimpinski K & Rice CL (2017). Electrophysiological and
481 neuromuscular stability of persons with chronic inflammatory demyelinating polyneuropathy.
482 *Muscle and Nerve* **56,** 413–420. DOI: 10.1002/mus.25516.

483 Di Girolamo FG, Fiotti N, Milanović Z, Situlin R, Mearelli F, Vinci P, Šimunič B, Pišot R, Narici M & Biolo
484 G (2021). The Aging Muscle in Experimental Bed Rest: A Systematic Review and Meta-Analysis.
485 *Front Nutr* **8,** 1–13. DOI: 10.3389/fnut.2021.633987.

486 Glover EI, Phillips SM, Oates BR, Tang JE, Tarnopolsky MA, Selby A, Smith K & Rennie MJ (2008).
487 Immobilization induces anabolic resistance in human myofibrillar protein synthesis with low
488 and high dose amino acid infusion. *J Physiol* **586,** 6049–6061. DOI:
489 10.1113/jphysiol.2008.160333.

490 Guo Y, Jones EJ, Inns TB, Ely IA, Stashuk DW, Wilkinson DJ, Smith K, Piasecki J, Phillips BE, Atherton PJ
491 & Piasecki M (2022). Neuromuscular recruitment strategies of the vastus lateralis according to
492 sex. *Acta Physiol*1–14. DOI: 10.1111/apha.13803.

493 Heckman CJ, Johnson M, Mottram C & Schuster J (2008). Persistent inward currents in spinal
494 motoneurons and their influence on human motoneuron firing patterns. *Neuroscientist* **14,**
495 264–275. DOI: 10.1177/1073858408314986.

496 Hourigan ML, McKinnon NB, Johnson M, Rice CL, Stashuk DW & Doherty TJ (2015). Increased motor

497 unit potential shape variability across consecutive motor unit discharges in the tibialis anterior
498 and vastus medialis muscles of healthy older subjects. *Clin Neurophysiol* **126,** 2381–2389. DOI:
499 10.1016/j.clinph.2015.02.002.

500 Hyngstrom AS, Johnson MD, Miller JF & Heckman CJ (2007). Intrinsic electrical properties of spinal
501 motoneurons vary with joint angle. *Nat Neurosci* **10,** 363–369. DOI: 10.1038/nn1852.

502 Jones EJ, Chiou S, Atherton PJ, Phillips BE & Piasecki M (2022). Ageing and exercise-induced motor
503 unit remodelling. *J Physiol* **600,** 1839–1849. DOI: 10.1113/jp281726.

504 Jones EJ, Piasecki J, Ireland A, Stashuk DW, Atherton PJ, Phillips BE, McPhee JS & Piasecki M (2021).
505 Lifelong exercise is associated with more homogeneous motor unit potential features across
506 deep and superficial areas of vastus lateralis. *GeroScience* **43,** 1555–1565. DOI:
507 10.1007/s11357-021-00356-8.

508 McFarland AJ, Ray PR, Bhai S, Levine BD & Price TJ (2022). RNA sequencing on muscle biopsy from a
509 5-week bed rest study reveals the effect of exercise and potential interactions with dorsal root
510 ganglion neurons. *Physiol Rep* **10,** 1–14. DOI: 10.14814/phy2.15176.

511 Mesquita RNO, Taylor JL, Trajano GS, Škarabot J, Holobar A, Gonçalves BAM & Blazevich AJ (2022).
512 Effects of reciprocal inhibition and whole-body relaxation on persistent inward currents
513 estimated by two different methods. *J Physiol* **0,** 1–23. DOI: 10.1113/jp282765.

514 Monti E, Reggiani C, Franchi M V., Toniolo L, Sandri M, Armani A, Zampieri S, Giacomello E, Sarto F,
515 Sirago G, Murgia M, Nogara L, Marcucci L, Ciciliot S, Šimunic B, Pišot R & Narici M V. (2021).
516 Neuromuscular junction instability and altered intracellular calcium handling as early
517 determinants of force loss during unloading in humans. *J Physiol* **599,** 3037–3061. DOI:
518 10.1113/JP281365.

519 Mulder ER, Stegeman DF, Gerrits KHL, Paalman MI, Rittweger J, Felsenberg D & de Haan A (2006).
520 Strength, size and activation of knee extensors followed during 8 weeks of horizontal bed rest
521 and the influence of a countermeasure. *Eur J Appl Physiol* **97,** 706–715. DOI: 10.1007/s00421-
522 006-0241-6.

523 Narici M V. & De Boer MD (2011). Disuse of the musculo-skeletal system in space and on earth. *Eur J*
524 *Appl Physiol* **111,** 403–420. DOI: 10.1007/s00421-010-1556-x.

525 Nuccio S, Del Vecchio A, Casolo A, Labanca L, Rocchi JE, Felici F, Macaluso A, Mariani PP, Falla D,
526 Farina D & Sbriccoli P (2021). Deficit in knee extension strength following anterior cruciate
527 ligament reconstruction is explained by a reduced neural drive to the vasti muscles. *J Physiol*
528 **599,** 5103–5120. DOI: 10.1113/JP282014.

529 Phillips SM, Glover EI & Rennie MJ (2009). Alterations of protein turnover underlying disuse atrophy
530 in human skeletal muscle. *J Appl Physiol* **107,** 645–654. DOI: 10.1152/japplphysiol.00452.2009.

531 Piasecki J, Inns TB, Bass JJ, Scott R, Stashuk DW, Phillips BE, Atherton PJ & Piasecki M (2021*a*).
532 Influence of sex on the age-related adaptations of neuromuscular function and motor unit
533 properties in elite masters athletes. *J Physiol* **599,** 193–205. DOI: 10.1113/JP280679.

534 Piasecki M, Garnés-Camarena O & Stashuk DW (2021*b*). Near-fiber electromyography. *Clin*
535 *Neurophysiol* **132,** 1089–1104. DOI: 10.1016/j.clinph.2021.02.008.

536 Piasecki M, Ireland A, Jones DA & McPhee JS (2016*a*). Age-dependent motor unit remodelling in
537 human limb muscles. *Biogerontology* **17,** 485–496. DOI: 10.1007/s10522-015-9627-3.

538 Piasecki M, Ireland A, Piasecki J, Stashuk DW, Swiecicka A, Rutter MK, Jones DA & McPhee JS (2018).
539 Failure to expand the motor unit size to compensate for declining motor unit numbers

distinguishes sarcopenic from non-sarcopenic older men. *J Physiol* **596,** 1627–1637. DOI: 10.1113/JP275520.

Piasecki M, Ireland A, Stashuk D, Hamilton-Wright A, Jones DA & McPhee JS (2016*b*). Age-related neuromuscular changes affecting human vastus lateralis. *J Physiol* **594,** 4525–4536. DOI: 10.1113/JP271087.

Puthucheary ZA et al. (2013). Acute skeletal muscle wasting in critical illness. *JAMA - J Am Med Assoc* **310,** 1591–1600. DOI: 10.1001/jama.2013.278481.

Rudrappa SS, Wilkinson DJ, Greenhaff PL, Smith K, Idris I & Atherton PJ (2016). Human skeletal muscle disuse atrophy: Effects on muscle protein synthesis, breakdown, and insulin resistance-A qualitative review. *Front Physiol* **7,** 1–10. DOI: 10.3389/fphys.2016.00361.

Scott JM, Martin DS, Ploutz-Snyder R, Matz T, Caine T, Downs M, Hackney K, Buxton R, Ryder JW & Ploutz-Snyder L (2017). Panoramic ultrasound: a novel and valid tool for monitoring change in muscle mass. *J Cachexia Sarcopenia Muscle* **8,** 475–481. DOI: 10.1002/jcsm.12172.

Stålberg E V. & Sonoo M (1994). Assessment of variability in the shape of the motor unit action potential, the “jiggle,” at consecutive discharges. *Muscle Nerve* **17,** 1135–1144. DOI: 10.1002/mus.880171003.

Stewart CR, Nandedkar SD, Massey JM, Gilchrist JM, Barkhaus PE & Sanders DB (1989). Evaluation of an automatic method of measuring features of motor unit action potentials. *Muscle Nerve* **12,** 142–148. DOI: 10.1002/mus.880120209.

Uncini A, Lange DJ, Lovelace RE, Solomon M & Hays AP (1990). Long-duration polyphasic motor unit potentials in myopathies: A quantitative study with pathological correlation. *Muscle Nerve* **13,** 263–267. DOI: 10.1002/mus.880130315.

Wall BT, Dirks ML, Snijders T, Senden JMG, Dolmans J & Van Loon LJC (2014). Substantial skeletal muscle loss occurs during only 5 days of disuse. *Acta Physiol* **210,** 600–611. DOI: 10.1111/apha.12190.

Zalewska E, Hausmanowa-Petrusewicz I & Stålberg E (2004). Modeling studies on irregular motor unit potentials. *Clin Neurophysiol* **115,** 543–556. DOI: 10.1016/j.clinph.2003.10.031.

Zalewska E, Szmidt-Salkowska E, Rowinska-Marcinska K, Kaminska A & Hausmanowa-Petrusewicz I (2013). Motor unit potentials with satellites in dystrophinopathies. *J Electromyogr Kinesiol* **23,** 580–586. DOI: 10.1016/j.jelekin.2012.11.002.